Three-dimensional sensing, imaging and recognition of objects having small number of photons

Inkyu Moon*[a] and Bahram Javidi[b]
[a]School of Computer Engineering, Chosun University,
375 Seosuk-dong, Dong-gu, Gwangju 501-759, South Korea;
[b]Dept. of Electrical and Computer Engineering, U-2157, University of Connecticut,
Storrs, CT USA 06269-2157

ABSTRACT

In this paper we overview the statistical method to three-dimensionally recognize very small number of photon-counted objects by using integral imaging (II). A conventional Poisson probability density function is assumed for modeling the distribution of very small number of photons count observation. For three-dimensional (3D) recognition of the small number of photon counted images, the photon limited elemental images set of a 3D object is obtained using the II technique. Then, the virtual geometrical ray propagation algorithm and the parametric maximum likelihood estimator are applied to the photon limited elemental image set in order to reconstruct the irradiance of the original 3D scene pixels. The sampling distributions for the statistical parameters of the reconstructed image are determined. Finally, hypothesis testing for the equality of the statistical parameters between reference and input data sets is performed for statistical classification of populations on the basis of sampling distribution information. Kolmogorov-Smirnov test is conducted and statistical p-value is measured. It is shown in experiments that very small number of photons counted image can be recognizable by the integral imaging and statistical sampling methods.

Keywords: Three-dimensional image processing, Three-dimensional image recognition, and Medical and biological imaging

1. INTRODUCTION

Integral imaging (II) has been investigated for three-dimensional (3D) sensing and visualization of objects over the last decade [1-9]. It has found a variety of applications including 3D object recognition, automatic analysis of 3D microscopic image data, and 3D display [10-12]. II is a 3D imaging technique based on integral photography. In this technique, multi-perspective information is obtained to extract the depth information of a 3D object. For 3D visualization of the object, the computational modeling of II is performed by using virtual ray propagation algorithm [11].

There are many benefits in developing photon-limited imaging systems [13] such as artificial compound eyes for visualization and detection of objects in extremely dark environment or low emission intensity. These photon-limited imaging systems can provide very significant power savings, high timing resolution, and recognition of photons-counted images. In addition, image information can be compressed with high compression ratio. Therefore, such systems can be used in various applications such as bio-medical imaging, data processing, and night vision.

In this paper we overview an imaging system which can provide 3D recognition of objects with a few photons [14]. We consider a Poisson probability density function for modeling the distribution of very small number of photons count observation. The II technique and maximum likelihood estimator are applied to sense and visualize the photon limited objects. For 3D recognition of objects with very small number of photons, statistical sampling algorithms are developed to be independent of the shape and profile of the photon counted objects. Kolmogorov-Smirnov (K-S) test is conducted in order to analyze the difference of the sampling histogram of two populations [15].

*inkyu.moon@chosun.ac.kr; phone 8262-230-0633

Enabling Photonics Technologies for Defense, Security, and Aerospace Applications V,
edited by Michael J. Hayduk, Peter J. Delfyett Jr., Andrew R. Pirich, Eric J. Donkor, Proc. of SPIE Vol. 7339,
733908 · © 2009 SPIE · CCC code: 0277-786X/09/$18 · doi: 10.1117/12.822118

The sections of this paper are as follows. Section 2 is an overview of the II and computational reconstruction. Section 3 explains a photon count model in II system and a 3D visualization of photon counted objects. The algorithms based on statistical inference are described for 3D recognition of the objects having very small number of photons in Section 4. Experimental results are illustrated in Section 5. Conclusions follow in Section 6.

2. PRINCIPLE OF INTEGRAL IMAGING AND COMPUTATIONAL RECONSTRUCTION

II is one of 3D imaging techniques in which directional information of a 3D object as well as the irradiance of the ray emanating from the 3D objects can be obtained. For 3D sensing of an object, the camera array or image sensor channels in the II system capture two-dimensional (2D) elemental images set having different perspectives of a 3D object. The perspective information varies according to the image channel position from the 3D object. The pickup process of II is illustrated in Fig. 1, where a simple model for the 3D scene consists of two planar objects placed at two different positions from the image plane. It is noted that the II having a synthetic aperture or camera array can be used to obtain the elemental images with high resolution since the II captures each elemental image by moving a CCD at corresponding position of each lenslet.

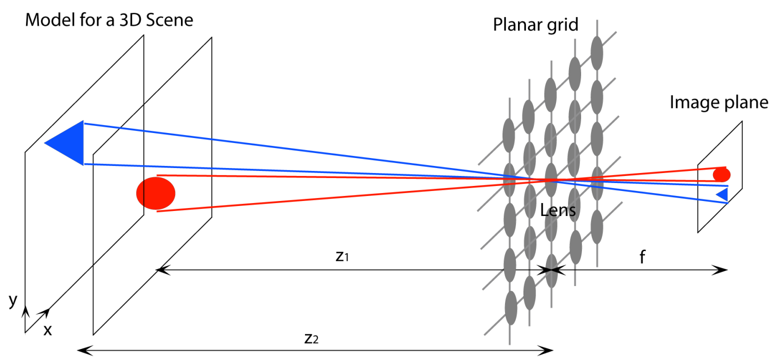

Fig. 1. Pickup process in integral imaging (II) having a synthetic aperture.

For computational reconstruction of a 3D object in II, it is possible to simulate the reverse of the pick-up process using geometrical optics [11]. In this method, a 2D plane of the 3D scene located at a particular distance is reconstructed by back propagating the captured elemental images on to that distance, through the simulated pinhole arrays as shown in Fig. 2. The ray back propagation algorithm consists of shifting and magnifying each elemental image with respect to the distance of the desired reconstruction plane and the location of its associated imaging device on the pick-up plane or image plane. Then the magnified elemental images overlap on the reconstruction plane such that the objects originally located at the reconstruction distance. Finally, the full 3D scene is obtained by producing all the 2D sectional images at the reconstruction depths. Therefore, in the computational II a 3D image reconstruction can be obtained since the overlapping factor in the elemental images is changed according to the reconstruction distance.

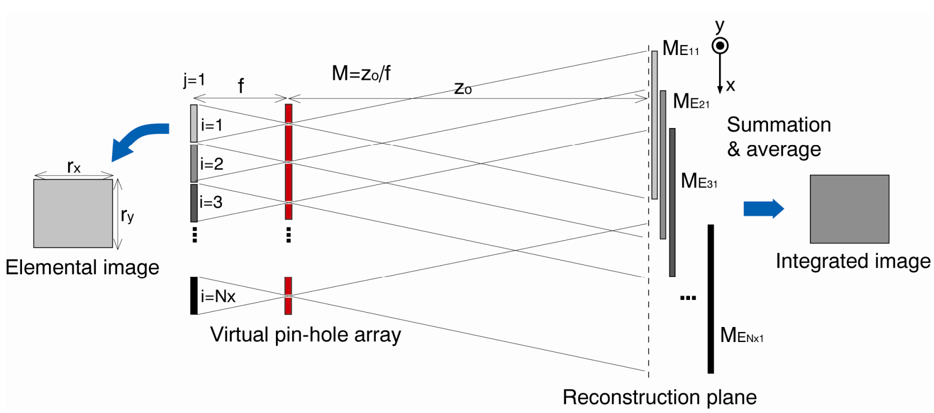

Fig. 2. Computational reconstruction in integral imaging (II).

3. PHOTON COUNTING INTEGRAL IMAGING FOR 3D VISUALIZATION OF PHOTON LIMITED OBJECTS

A Poisson model is applied for estimating the distribution of the discrete photon count observation. If the observed signal is based on light, then each photon of the light carries an energy hυ, where h denotes Plank's constant and υ is the mean frequency of a light. The probability for photon counting at an observation area or a pixel during exposure time interval follows Poisson distribution [16]. In II system, an array of regular square elements with uniform size is shown in Fig. 1. The array is illuminated by a photon beam such that the irradiance at the one pixel point of a 3D object is recorded on the corresponding one pixel position of each elemental image, where all the pixel positions are calculated by geometrical ray optics. The values of such pixels are assumed as a random variable following a Poisson density function.

Equation (1) denotes a probability density function with a constraint on the total number of photons detected by each sensor. Therefore the photon limited images from the irradiance images according to the Eq. (1) can be simulated [14].

$$\Pr(C_x \mid \rho_x) = \frac{[\rho_x]^{C_x} e^{-\rho_x}}{C_x!}, \quad \sum_{x=1}^{N_T} \rho_x = 1, \tag{1}$$

where ρ_x is normalized irradiance at an observation area or a pixel x during an exposure time, N_T is the total number of pixels of the elemental image and a random variable C_x has values 0, 1, 2, · · ·. We assumed that the Poisson parameter for the photon counts at each pixel in the photon limited image is proportional to the irradiance of the pixel in elemental image. In order to generate a photon limited elemental image having N_p number of photons on the average, the following Poisson distribution function with the mean parameter $\rho_x N_p$ at each pixel of the irradiance image can be given by:

$$\Pr(C_x \mid \rho_x N_p) = \frac{[\rho_x N_p]^{C_x} e^{-\rho_x N_p}}{C_x!} \sim Poisson(\rho_x N_p). \tag{2}$$

For 3D visualization of the photon limited object, the generated photon limited elemental images set is back propagated on to arbitrary position at the reconstruction depths, through the simulated pinhole arrays. Finally computational 3D reconstruction of the objects having small number of photons is obtained.

4. STATISTICAL INFERENCE FOR 3D RECOGNITION OF PHOTON LIMITED OBJECTS

In this section, the statistical method for 3D recognition of objects having small number of photons is described. A nonparametric statistical test is used for comparison of two data histograms. Statistical sampling theory [17] is useful tool in determining whether the observed differences between two sampling data sets are significant. For statistical decision, a hypothesis test can be performed by constructing the statistical sampling distribution of a test statistic.

In order to obtain the statistical sampling distribution of the test statistic, the integrated image n times by using the computational II reconstruction algorithm is reconstructed. Let II_p^i denote the i^{th} integrated image reconstructed from the corresponding photon-limited elemental images set, where the photon-limited elemental image is generated with a random number of photons. The statistical sampling distribution of the dispersion parameter for the reconstructed integrated image is obtained by calculating the statistical standard deviation of the each II_p^i, where $i = 0,\ldots,n$. Then, given n ordered data samples $X(1), X(2), \cdots X(n)$ the empirical cumulative density function (ECDF) for the statistical distribution is calculated. A statistical K-S test [15] is applied for 3D recognition of the objects having small number of photons. The statistical method calculates the maximum distance between the calculated empirical cumulative distribution functions (ECDF) of true class reference and unknown input data histograms for a statistical parameter.

For statistical decision about populations on the basis of statistical sampling distribution information, we set a null hypothesis $\mathrm{H}_0 : F^r(u) = F^i(u)$ for all u and alterative hypothesis $\mathrm{H}_1 : F^r(u) \neq F^i$ for at least one u, where $F^r(u)$ and $F^i(u)$ are ECDFs for reference and input data. Finally, we compute the statistical p-value of the K-S test statistics.

5. EXPERIMENTAL RESULTS

An II system with camera array is shown in Fig. 3, where the two toy cars were used in the experiments. The toy cars were illuminated with a white light. In order to evaluate the presented 3D recognition system, we recorded an object's elemental images set by moving a CCD camera transversally in both x and y directions. The resolution of image sensor array is a 2028×2044 and has a pixel size of 9μm×9μm. The 10×10 elemental images were captured. It is noted that the elemental images set on dynamic scenes can be captured with a single exposure by building a multiple video camera system [18].

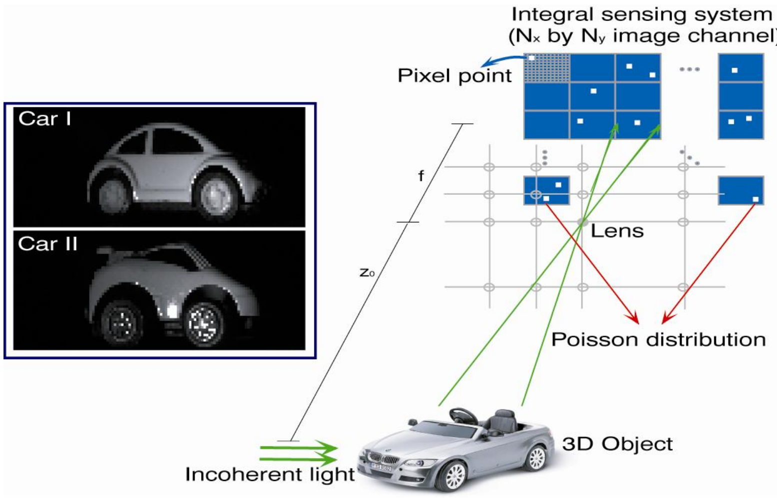

Fig. 3. Schematic setup of II system with camera array for 3D object visualization and recognition.

Figure 4 shows the sectional images of the 3D scenes for the car I and II reconstructed by using computational II algorithm, respectively. The cars were reconstructed at distance z_0 = 100cm. The photon-counted elemental images of the car I and II were generated according to a photon counting detection model. Figure 5 shows the subset of the elemental images of the car I and II with a single photon per elemental image, respectively. In Fig. 6 we show the sectional images of the 3D scenes for the car I and II, respectively. The sectional images are reconstructed at distance z_0 = 100cm with the corresponding photon-counted elemental images set, where we set the expected number of photons with $\tilde{N}$ =1, 11, and 51.

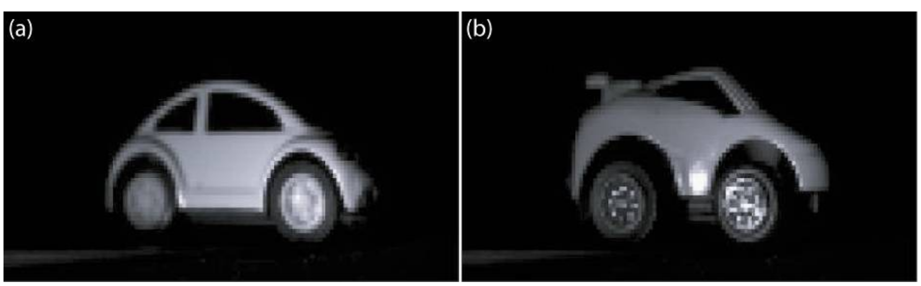

Fig. 4. Sectional 3D image reconstruction at distance z_0 =100cm with 10×10 elemental images set, where the size of the reconstructed image is 150×100 pixels. (a) car I and (b) car II.

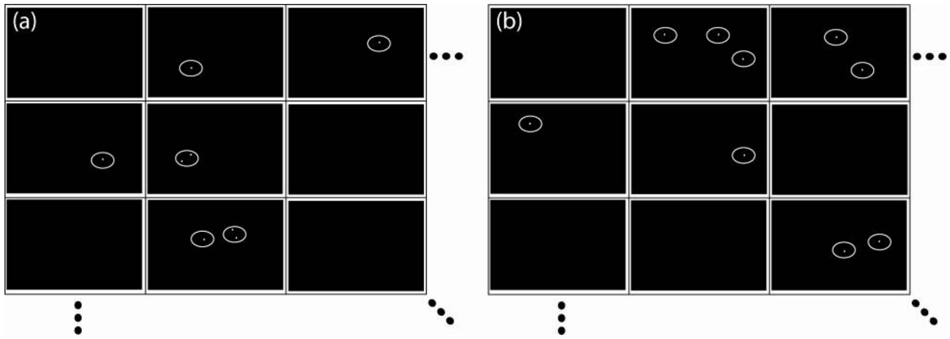

Fig. 5. Subset of elemental images having small number of photons generated according to a photon counting detection model. (a) car I and (b) car II.

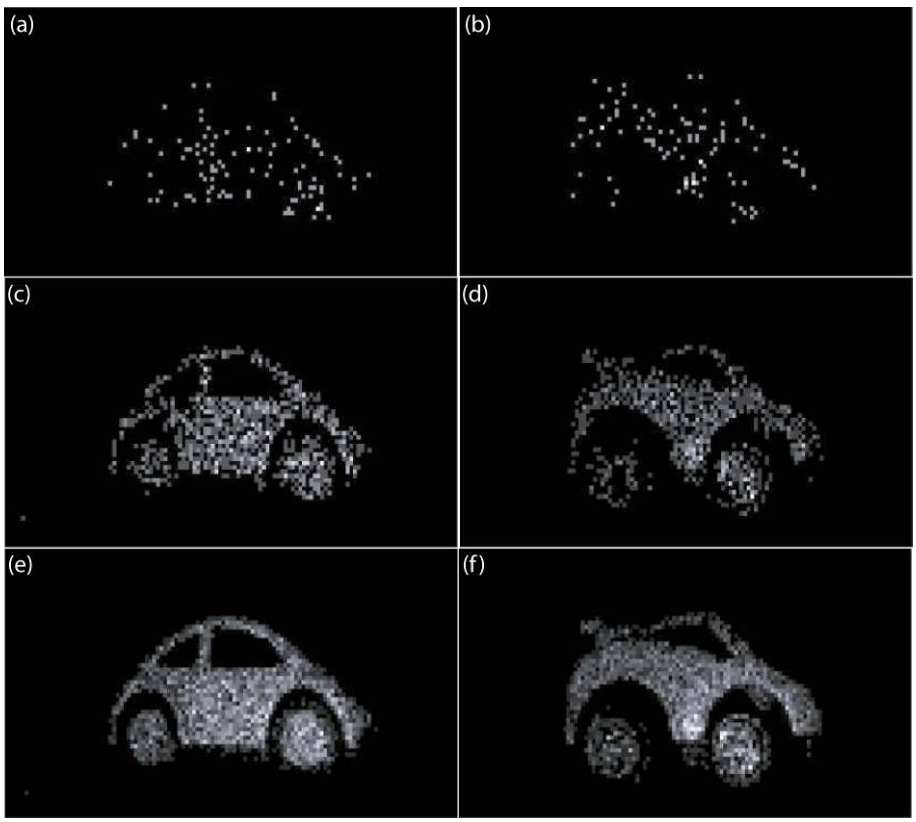

Fig. 6. Sectional images of the 3D scenes reconstructed from very small number of photons-counted elemental images, where the 10×10 elemental images set was generated with the photon counting detection model. $\tilde{N}$ is the expected number of photons per elemental image. (a) Car I with $\tilde{N}$ =1, (b) Car II with $\tilde{N}$ =1, (c) Car I with $\tilde{N}$ =11, (d) Car II with $\tilde{N}$ =11, (e) Car I with $\tilde{N}$ =51, (f) Car II with $\tilde{N}$ =51.

It can be considered from Fig. 5 that recognizing the two-dimensional (2D) image with very small number of photons is not easy work even if many a single photon counted 2D images for a target object can be obtained at one exposure. However, it can be possible to recognize the target object having very low number of photons by use of the sectional images of the 3D scene reconstructed from the II technique if sufficient number of elemental images can be captured. The reconstructed image results are statistically analyzed in order to inspect the possibility of the 3D recognition of the objects with a very small number of photons. We first computationally reconstruct one sectional image of photon counting 3D scene located at distance z_0 = 100cm from the sensor using the photon-limited elemental images set. The process is repeated 100 times and each time the statistical standard deviation of the reconstructed sectional image is computed. We define the computed statistical standard deviation as random variable σ. As a result, we have 100 samples for the random variable σ and the statistical sampling distribution or histogram for the random variable is formed.

The statistical K-S test is performed to compare the two histograms between reference and input data sets of known reference car I and unknown input data car II to perform the statistical decision. The K-S statistic tests the null hypothesis ($\mathrm{H}_0 : F^r(u) = F^i(u)$) that the two histograms follow the same distributions using a level of significance. Figure 7 shows the computed K-S test p-value and the test statistic value versus the expected number of photons for the random variables σ, where we have changed the expected number of photons from $\tilde{N}$ =1 to $\tilde{N}$ =51 with an interval of 5. As shown in Fig. 5, it is noted that when elemental images counted with only a single photon were used, the statistical p-value computed for random variable σ was 9.937×10^{-2}. It means that the test statistic discriminates between the two different data sets (car I and car II) with approximately 90.1% accuracy. And, most of the p-values in Fig. 7 for comparing the two histograms or statistical sampling distributions of the random variable σ were less than 0.005. It is noted that the statistical p-value computed for the equality of two histograms of the random variable σ significantly decreases when the expected number of photons increase. Clearly, the test statistic for random variable σ discriminates between the two different data sets (car I and car II) with over 99.9% accuracy in the range of the expected number of photons $6 \le \tilde{N} \le 51$, where the sample size was 100.

Figure 8 show the cumulative density function plots of the statistical sampling distributions of known reference car I and unknown input data car II for the random variable σ, where the total number of elemental images was 100 and we set the expected number of photons with $\tilde{N}$ =11 and 51. As expected, the graphs (a) and (b) show there is large K-S distance Λ between two different data sets. Therefore, the graphs lead to the conclusion that there is a large dissimilarity between two different classes (car I and car II). Note that the separation or the K-S distance of two different datasets increases when the expected number of photons $\tilde{N}$ increases.

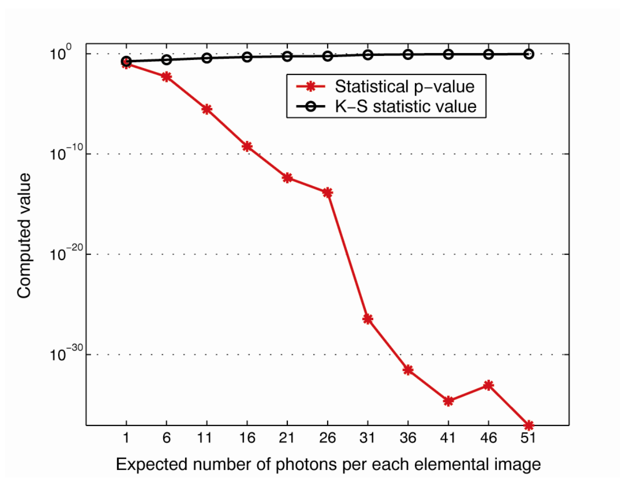

Fig. 7. Experimental results of the K-S test for checking the equality of two histograms of the reference car I and unknown input data car II. The histograms are determined for random variable σ. The measurements are performed versus the expected number of photons $\tilde{N}$. The expected number of photons was changed from $\tilde{N}$ =1 to $\tilde{N}$ =51 with an interval of 5 and the total number of elemental images was 100.

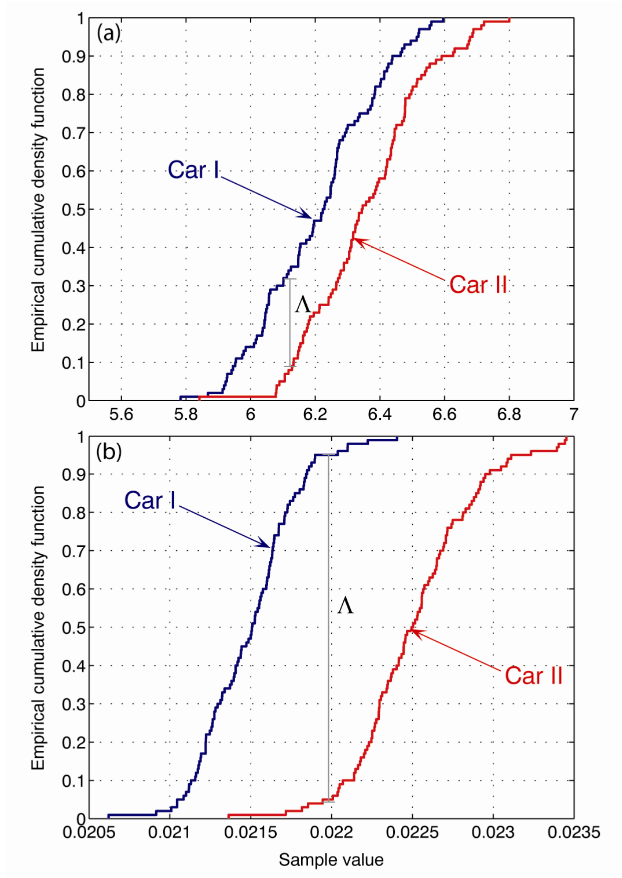

Fig. 8. Cumulative density function plots of the statistical sampling distributions of the reference car I and unknown input data car II for the random variable σ, where the total number of elemental images was 100. (a) $\tilde{N}$ =11 and (b) $\tilde{N}$ =51.

6. CONCLUSIONS

In this paper, we have overviewed a method to provide the 3D recognition of small number of photons counted objects. Our approach is based on an integral imaging (II), a parametric maximum likelihood estimator, and statistical inference algorithms. Using II techniques, the elemental images of a 3D object are captured from different perspectives. The single or a few photon limited elemental images are generated by a photon-counting detection model.

For 3D visualization and recognition of the objects with small number of photons, the integrated image of a 3D scene is estimated using parametric MLE on the photon-counts modeled by a Poisson density function. And then, statistical inference algorithms are applied for a statistical decision about populations on the basis of statistical sampling distribution information.

We have presented experiments in order to verify the presented method and analyzed the integrated images measuring statistical properties. It was shown that a few photons counted objects can be three-dimensionally recognizable by the sectional images of the 3D scene reconstructed using the computational II if sufficient number of elemental images can be captured. In addition, the data compression and dimensionality reduction of the photon counted elemental images set can be achievable. A further image processing and advanced pattern recognition algorithms can be applied to the sectional images of the 3D scene in order to increase the 3D object recognition performance.

REFERENCES

[1] B. Javidi and F. Okano, eds., Three-Dimensional Television, Video, and Display Technologies (Springer, Berlin, 2002).

[2] T. Okoshi, ed., Three-Dimensional Imaging Techniques (Academic Press, 1976).

[3] G. Lippmann, "La photographie intégrale," Compte-Rendus 146, 446-451 (1908).

[4] H. Hoshino, F. Okano, H. Isono, and I. Yuyama, "Analysis of resolution limitation of integral photography," J. Opt. Soc. Am. A 15, 2059-2065 (1998).

[5] A. Stern and B. Javidi, "Three-dimensional image sensing, visualization, and processing using integral imaging," Proc. IEEE 94, 591-607 (2006).

[6] S. Benton, ed., Selected Papers on 3D Displays (SPIE Press, Bellingham, WA, 2001).

[7] A. Castro, Y. Frauel, and B. Javidi, "Integral imaging with large depth of field using an asymmetric phase mask," Opt. Express 15, 10266-10273 (2007).

[8] Y. Igarishi, H. Murata, and M. Ueda, "3D display system using a computer-generated integral photograph," Jpn. J. Appl. Phys. 17, 1683-1684 (1978).

[9] P. Sokolov, ed., Autostereoscpy and Integral Photography by Professor Lippmann's Method (Moscow State Univ. Press, Moscow, Russia, 1911).

[10] O. Matoba, E. Tajahuerce, and B. Javidi, "Real-time three-dimensional object recognition with multiple perspectives imaging," Appl. Opt. 40, 3318-3325 (2001).

[11] Y. Hwang, S. Hong, and B. Javidi, "Free view 3-D visualization of occluded objects by using computational synthetic aperture integral imaging," J. Display Technol. 3, 64-70 (2007).

[12] R. Martínez-Cuenca, G. Saavedra, M. Martínez-Corral, and B. Javidi, "Extended depth-of-field 3-D display and visualization by combination of amplitude-modulated microlenses and deconvolution tools," J. Display Technol. 1, 321- 327 (2005).

[13] E. Watson and G. Morris, "Comparison of infrared up conversion methods for photon-limited imaging," J. Appl. Phys. 67, 6075-6084 (1990).

[14] I. Moon and B. Javidi, "Three-dimensional recognition of photon starved events using computational integral imaging and statistical sampling," Opt. Lett. 34, 731-733 (2009).

[15] M. Hollander and D. Wolfe, eds., Nonparametric Statistical Methods (Wiley, 1999).

[16] J. Goodman, ed., Statistical Optics, (John Wiley & Sons, Inc. 1985).

[17] N. Mukhopadhyay, ed., Probability and Statistical Inference (Marcel Dekker, Inc. New York, 2000).

[18] M. Levoy, "Light fields and computional imaging," IEEE Computer 46-55 (2006).